ELSEVIER

Journal of Chromatography A, 765 (1997) 307–314

JOURNAL OF CHROMATOGRAPHY A

Theory concerning the current for an end-column amperometric detector with a disk working electrode in capillary zone electrophoresis

Wenrui Jin*, Haifeng Chen

Laboratory of Analytical Science, School of Chemistry, Shandong University, Jinan 250100, China

Received 16 August 1996; revised 1 November 1996; accepted 1 November 1996

Abstract

The equations for the current curve [i.e. the relationship between current detected (A), i, and the time, t (s)] and its peak current, i_p (A), for an end-column amperometric detector with a disk working electrode in capillary zone electrophoresis have been investigated and can be expressed as follows:

$$i = \frac{1}{2}nFcU\left[1 - m_1\exp\left(-\frac{m_2DA}{Ub}\right)\right]\left[\operatorname{erf}\frac{\frac{L_i}{2} - (l - v_m t)}{2\sqrt{Dt}} + \operatorname{erf}\frac{\frac{L_i}{2} + (l - v_m t)}{\sqrt{Dt}}\right]$$

and

$$i_p = nFcU\left[1 - m_1\exp\left(-\frac{m_2DA}{Ub}\right)\right]\operatorname{erf}\frac{L_i}{4\sqrt{Dt_m}}$$

where D is the diffusion coefficient of the species detected (cm^2/s), A is the area of the disk working electrode (cm^2), U is the average volumetric velocity (cm^3/s), b is the distance between the electrode and the capillary outlet (cm), c is the concentration of the species detected in solution (mol/cm^3), L_i is the injection length (cm), l is the distance between the detector and the capillary inlet (cm), v_m is the migration velocity (cm/s), t_m is the migration time (s) at which the current detected has a maximum value, n and F have their normal significance. m_1 and m_2 are constants, which can be determined experimentally.

Both equations have been verified experimentally.

Keywords: Detection, electrophoresis; Amperometric detection; Cysteine

1. Introduction

Capillary zone electrophoresis (CZE) has been introduced as a rapid highly efficient technique for the separation of ionized solutes [1–3]. Although on-column UV detection is the most popular detection method in CZE, the sensitivity of the method is poor due to the small path length of the fused-silica capillary. In addition, the wavelength used in UV detection lacks the necessary selectivity for biological samples. Laser fluorescence detectors provide the necessary sensitivity for CZE. However,

*Corresponding author.

PII S0021-9673(96)00973-9

laser-induced fluorescence detection often requires pre- or post-column derivatization of the sample of interest. Amperometric detection with microelectrodes, introduced first by Wallingford and Ewing [4], has been shown to be one of the most sensitive detection techniques available for use with microcolumn liquid-phase separations [5–8]. The first design for amperometric detection is called off-column amperometric detection. Its main feature is the use of an electrically conductive joint between the separation capillary and the detection capillary, which is made by placing a small fracture near the cathodic end of the separation capillary and covering the crack with a porous glass [9,10], porous graphite tube [11], Nafion tubing [12,13], cellulose acetate-coated porous polymer [14], Nafion film [15,16] and PTFE tubing [17], in order to decouple the electrochemical detector from the high separation voltage. The working microelectrode is inserted into the detection end of the detection capillary column. This kind of amperometric detector is not convenient for at least two reasons: it needs a conductive joint and the working microelectrode must be inserted into the detection capillary. More recently, new equipment for CZE–amperometric detection, called an end-column amperometric detector, has been described [18], in which the electrically conductive joint is not used and the working electrode is directly placed at the outlet of the separation capillary (i.e. it is not inserted into the capillary). Lu et al. [19,20] have investigated the characteristics of this type of end-column amperometric detector in detail. Their coulometric efficiency is slightly less than that of the off-column amperometric detector [21]. In this design, microsize working electrodes were employed, typically wires or fibers that were 5–50 μm in diameter and 100–150 μm in length. This requirement, in order to match the electrode size to that of the separation capillary (usually 25 μm I.D.), greatly complicates electrode fabrication and makes electrode/capillary alignment difficult to maintain, both during an electrophoretic run and from run to run. Ye and Baldwin [22] used a normally sized working electrode in the end-column amperometric detector without introducing significant post-capillary zone broadening. This type of design is convenient for the alignment of the electrode and the capillary. Usually, the electrode is a microcylinder, i.e. the electrode material protrudes from the isolated tubing, such as a glass tubing pipet tip (Fig. 1a). This mode makes the working electrode susceptible to being broken or bent and severely limits the experimenter's choice of possible electrode materials. Another design with a normal-sized microdisk working electrode is illustrated in Fig. 1b. Advantages of this type of end-column amperometric detector are its easy manufacture, convenient operation and lack of a limitation for electrode materials. They have been applied in CZE for amperometric detection with a carbon fiber array electrode [23], a chemically modified carbon paste electrode [24], a copper electrode [25] and a chemically modified gold array electrode [26].

This paper presents the theoretical equations for

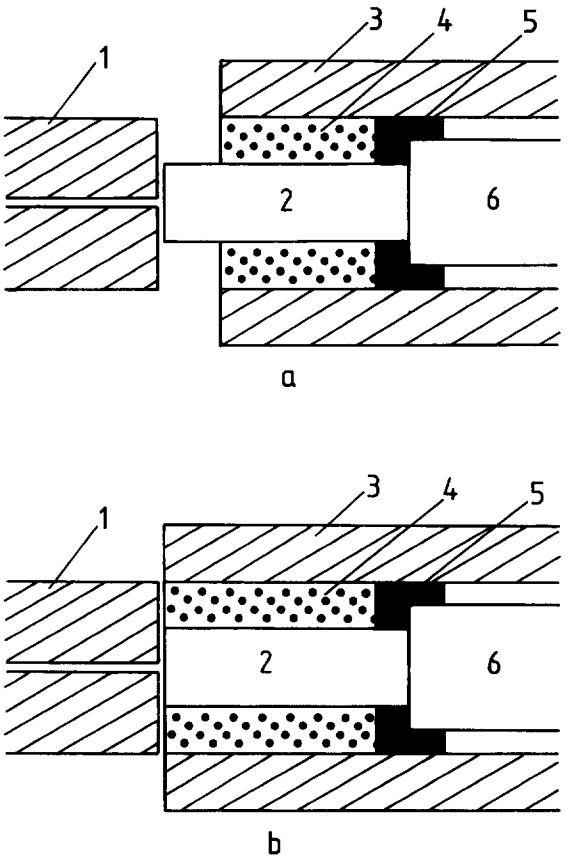

Fig. 1. Top view of the end-column amperometric detector (a) with a normal cylinder electrode and (b) with a normal disk electrode. 1 = Separation capillary; 2 = working electrode material; 3 = isolated tubing; 4 = epoxy glue; 5 = electrically conductive junction and 6 = copper wire.

the current curve (electropherogram) and its peak current for this type of end-column amperometric detector in CZE, which has not been reported to date, and which has been verified experimentally using L-cysteine for a gold–mercury amalgam electrode.

2. Theory

We shall assume that the zone broadening is only caused by the axial diffusion of ionized species. In CZE, the center of the zone should move with a velocity, v_m (migration velocity; cm/s), therefore, the distribution of the one-dimensional concentration, $c(l,t)$, of the species expected at time t(s) and at l (cm) (the distance between the detector and the capillary inlet), which is equal to the length of the capillary in usual cases, can be written as follows [27]

$$c(l,t)=\frac{c}{2}\left[\operatorname{erf}\frac{\frac{L_i}{2}-(l-v_m t)}{2\sqrt{Dt}}+\operatorname{erf}\frac{\frac{L_i}{2}+(l-v_m t)}{2\sqrt{Dt}}\right] \quad (1)$$

where D is the diffusion coefficient of the species (cm^2/s), L_i is the injection length (cm) and c is the initial concentration of the species (mol/cm^3).

For the end-column amperometric detector shown in Fig. 2, the solution flows off from the end of the capillary with fully developed laminar flow parallel to the electrode surface. The flow profile is similar to that of a rectangular open-channel electrode. Therefore, the coulometric efficiency of the end-column amperometric detector, η, can be written as [28,29]

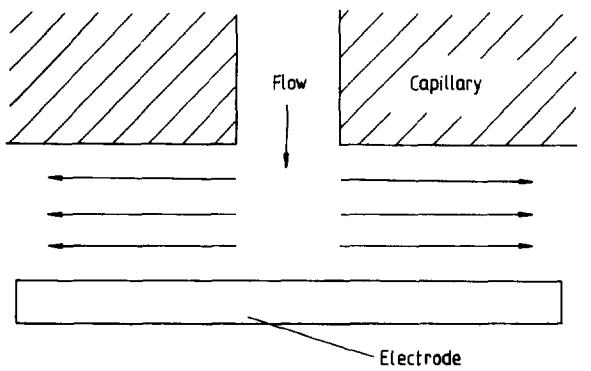

Fig. 2. Schematic representation of the flow profile for the end-column amperometric detector in CZE.

$$\eta=1-m_1\exp\left(-\frac{m_2DA}{Ub}\right) \quad (2)$$

where U is the average volume flow velocity of the fluid (cm^3/s), b is the distance between the electrode and the capillary outlet (cm), A is the area of the disk working electrode and m_1 and m_2 are constants that can be determined experimentally.

According to the definition of η, the relationship between the current detected at the end-column amperometric detector, i, and η may be expressed as

$$i=nFc(l,t)U\eta \quad (3)$$

where n and F have their usual meaning.

Substituting Eq. (2) into Eq. (3), we have

$$i=nFUc(l,t)\left[1-m_1\exp\left(-\frac{m_2DA}{Ub}\right)\right] \quad (4)$$

By combining Eqs. (1,4), we get

$$i=\frac{1}{2}nFcU\left[1-m_1\exp\left(\frac{m_2DA}{Ub}\right)\right]\times\left[\operatorname{erf}\frac{\frac{L_i}{2}-(l-v_m t)}{2\sqrt{Dt}}+\operatorname{erf}\frac{\frac{L_i}{2}+(l-v_m t)}{2\sqrt{Dt}}\right] \quad (5)$$

By differentiating Eq. (5) with respect to t and taking $di/dt=0$, $t=t_m=l/v_m$ is obtained (see Appendix A), which means that when $t=t_m$ (migration time), i is at its maximum, i.e. peak current, i_p.

Substituting $t=t_m=l/v_m$ into Eq. (5), the following equation for peak current, i_p, can be obtained

$$i_p=nFcU\left[1-m_1\exp\left(-\frac{m_2DA}{Ub}\right)\right]\operatorname{erf}\frac{L_i}{4\sqrt{Dt_m}}=nFcU\left[1-m_1\exp\left(-\frac{m_2\pi DR^2}{Ub}\right)\right]\operatorname{erf}\frac{L_i}{4\sqrt{Dt_m}} \quad (6)$$

where R is the radius of the working electrode (cm).

3. Experimental

3.1. Apparatus

A reversible high-voltage power supply (Beijing

Institute of New Technique, China) provided a variable voltage of 0–30 kV across the capillary with the outlet of the capillary at ground potential. Polyimide-coated fused-silica capillaries (300×25 μm I.D.) were purchased from Yongnian Optical Conductive Fiber Plant, China. Amperometric detection at a constant potential with CZE was performed using the end-column approach and a microcurrent voltammeter (Model 901-PA, Ningde Analytical Instruments, China). A piece of capillary was cut to the desired length. A small section (ca. 0.5 cm) of the polyimide coating at the end of the capillary was removed using a flame. The end of the capillary was ground and polished using emery paper. The capillary was positioned in the Plexiglass electrochemical cell. The detection cell and the detector were housed in a faradaic cage in order to minimize interference from external sources of noise. Electrochemical detection was carried out with a three-electrode system, which consisted of a coiled Pt wire (0.5 mm diameter, 4 cm in length) as the auxiliary electrode, which was placed at the bottom of the cell. This electrode also served as the ground for potential drop across the capillary. A saturated calomel electrode (SCE) was used as the reference electrode and a gold–mercury amalgam microelectrode was used as the working electrode.

The gold–mercury amalgam microelectrode was constructed using gold wires that were 100, 176, 230 and 300 μm in diameter, and ca. 7 cm long. This was inserted carefully through a ca. 0.4 mm I.D., 0.8 mm O.D. and 4 cm long glass capillary until it protruded approximately 2 cm from the end. Using a microscope, epoxy resin was then applied to the junction of the glass capillary to seal the fine gold wire to it. A copper wire was gummed to the outside of the other end of the glass capillary with epoxy resin. Then the gold wire was bound to the copper wire. In order to protect the electrical junction, the copper wire and the glass capillary were bound together with a piece of rubberized fabric. After the protrusion of the gold electrode had been ground into a plane, it was polished with emery paper first. The gold electrode was then washed with water, ethanol and double distilled water. The gold–mercury amalgam was prepared by dip-coating, i.e. the gold wire was dipped into pure mercury for approximately 45 s. Before experiments the old amalgam was removed and fresh amalgam was prepared using the dip-coating method.

The gold wires, with diameters of 176 and 230 μm, were obtained by etching gold wires with diameters of 300 μm with a solution containing 50 g/l I_2 and 200 g/l KI. The gold wires were then cleaned three times with concentrated HNO_3, water and acetone, respectively.

3.2. Reagents and solutions

A 0.02 mol/l stock solution of L-cysteine was prepared by dissolving an appropriate amount of L-cysteine (content >98.5%, Shanghai Kangda amino-acid factory, China) in 1 g/l ethylene diamine tetraacetic acid (disodium salt) (Na_2EDTA) solution and was stored at 4°C in a refrigerator. Dilute solutions were obtained by serially diluting the stock solution with the electrophoresis buffer ($6.1 \cdot 10^{-3}$ mol/l Na_2HPO_4–$3.9 \cdot 10^{-3}$ mol/l NaH_2PO_4). Other reagents were of analytical grade. All solutions were prepared using double distilled water.

3.3. Procedure

To prepare a CZE–amperometric detection system, the gold–mercury amalgam electrode was cemented onto a microscope slide, which was placed over an XYZ micromanipulator and glued in place, so that the end containing the exposed gold–mercury amalgam protruded from the edge of the slide. The position of the gold–mercury amalgam electrode was adjusted (under a microscope) to the end of the capillary. The other end of the capillary was inserted into a plastic syringe tip (the metal needle having been removed previously) and was glued in place with a small amount of epoxy glue. Before each run, the capillaries were flushed with double distilled water for 5 min and then with the corresponding separation electrolyte for 5 min using a syringe. In addition, the electrolyte solution in the electrochemical cell was replaced before each run. During the experiments, a separation voltage was applied across the capillary and the detection potential was applied at the working electrode. After the electroosmotic current reached a constant value (about 5 min), the electromigration injection was carried out and the electropherogram was recorded. In our experiments,

a 29-cm long capillary, $6.1\cdot10^{-3}$ mol/l Na_2HPO_4–$3.9\cdot10^{-3}$ mol/l NaH_2PO_4 buffer, pH 7.0 and a detection potential, E_d, of 0.09 V vs. SCE were used.

4. Results

The electrochemical behaviour of L-cysteine at a mercury electrode has been reported [30,31]. L-Cysteine (RSH) can be oxidized at the mercury electrode at a lower oxidation potential according to the following scheme:

$$2(RSH)_{soln} + Hg - 2H^+ - 2e^- \rightleftharpoons (Hg(RS)_2)_{ads} \quad (7)$$

The reaction is reversible and has been used in the determination of cysteine by CZE with end-column amperometric detection at a gold–mercury amalgam electrode [13,32]. In these experiments using CZE for determination of L-cysteine, it was demonstrated that there is no adsorption of L-cysteine on the wall of the fused-silica capillary in NaH_2PO_4–Na_2HPO_4 buffer, pH 7. In addition, the surface of the gold–mercury amalgam electrode can be measured accurately and made reproducibly. Therefore, the system (oxidation of L-cysteine in NaH_2PO_4–Na_2HPO_4 buffer, pH 7, at a gold–mercury amalgam electrode) is very suitable for the theoretical verification of the current curve and the peak current of the end-column amperometric detector.

In previous work [29], values for m_1 and m_2 of 0.94 and 0.41, respectively, were obtained in Eqs. (5,6), for the oxidation of L-cysteine at the gold–mercury amalgam electrode in CZE using the relationship of η and DA/Ub, as shown in Eq. (2), at different values of A, U and b.

4.1.1. Current curve (electropherogram)

Values of t_m, v_m, U and L_i at different values of V_s (separation voltage), V_i (injection voltage) and t_i (injection time) are listed in Table 1. The parameters v_m, U and L_i were calculated according to the following equations, respectively,

$$v_m = \frac{l}{t_m} \quad (8)$$

$$U = \frac{\pi a^2 l}{4 t_m} \quad (9)$$

Table 1
Experimental parameters of current curves in CZE

V_s (kV)	V_i (kV)	t_i (s)	t_m (s)	v_m (cm/s)	L_i (cm)	$10^6\ U$ (cm^3/s)
3	3	3.21	516	0.0562	0.181	0.276
6	6	1.84	257	0.113	0.208	0.554
9	9	1.32	170	0.171	0.225	0.836
12	12	1.17	126	0.230	0.270	1.130

Experimental conditions: $6.1\cdot10^{-3}$ mol/l Na_2HPO_4–$3.9\cdot10^{-3}$ mol/l NaH_2PO_4 (pH=7.0); $1.00\cdot10^{-4}$ mol/l L-cysteine. l=29.0 cm, a=25 μm, $R=5.00\cdot10^{-3}$ cm, b=20 μm, E_d (detection potential)=0.09 V vs. SCE.

and

$$L_i = \frac{V_i t_i l}{V_s t_m} \quad (10)$$

where a is the inner diameter of the capillary (cm).

Fig. 3 shows the experimental and theoretical electropherograms at different values of V_s, V_i and t_i. From these figures, it can be seen that the theoretical curves are in agreement with the experimental ones.

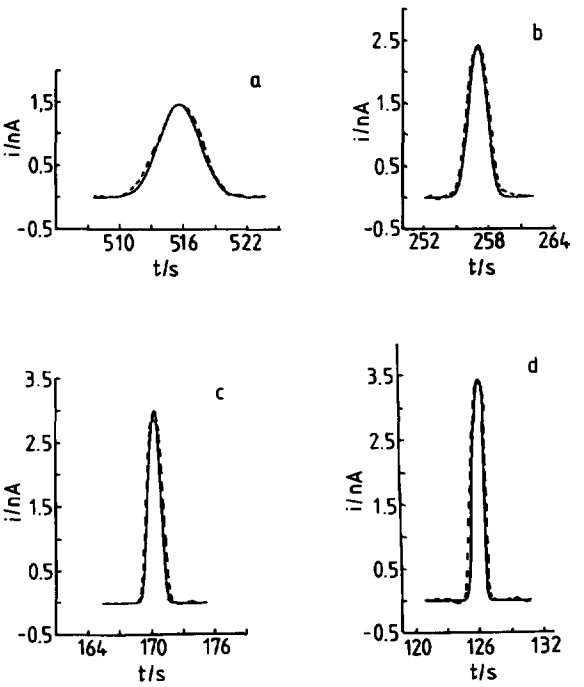

Fig. 3. Experimental (- - -) and theoretical (——) current curves (a) V_s=3 kV, V_i=3 kV and t_i=3.21 s; (b) V_s=6 kV, V_i=6 kV and t_i=1.84 s; (c) V_s=9 kV, V_i=9 kV and t_i=1.32 s; (d) V_s=12 kV, V_i=12 kV, t_i=1.17 s. Other conditions as in Table 1.

Table 2
Values of t_m, i_p and U at different values of V_s

V_s (kV)	t_m (s)	i_p (nA)	$10^6\ U$ (cm^3/s)
3	516	0.51	0.276
6	257	0.90	0.554
9	170	1.32	0.836
12	126	1.65	1.130

Experimental conditions: $V_i = 1$ kV, $t_i = 3.0$ s.
Other conditions as in Table 1.

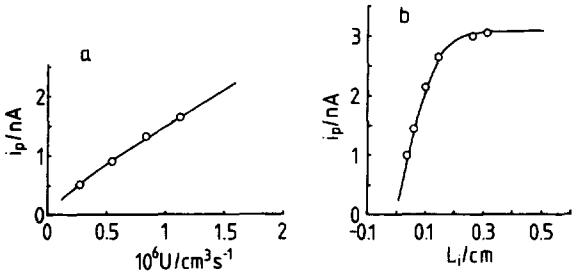

Fig. 4. Experimental (○) and theoretical (—) dependence of i_p on (a) U and (b) L_i. Conditions for (a) as in Table 2 and those for (b) as in Table 3.

4.1.2. Peak current

Determined values of t_m and i_p and calculated values of U at different V_s values are listed in Table 2. The experimental values of i_p at different values of U and the theoretical curve of $i_p \sim U$ are shown in Fig. 4a. Determined values of t_m and i_p and calculated values of L_i at different t_i are listed in Table 3. The experimental values of i_p at different L_i and the theoretical curve of $i_p \sim L_i$ are shown in Fig. 4b.

Fig. 5 shows the experimental values of i_p at different b, R and c and the theoretical curves of $i_p \sim b$, $i_p \sim R$ and $i_p \sim c$. From these figures it can be seen that the experimental values are in agreement with the theoretical curves. These experimental results indicate that Eqs. (5,6) are correct.

Table 3
Values of t_m, i_p and L_i at different values of t_i

t_i (s)	t_m (s)	i_p (nA)	L_i (cm)
1.00	170	1.00	0.0378
1.51	170	1.65	0.0571
2.58	170	2.15	0.0976
3.90	170	2.66	0.148
6.92	170	2.92	0.262
8.30	170	3.05	0.314

Experimental conditions: $V_s = 9$ kV, $V_i = 2$ kV.
Other conditions as in Table 1.

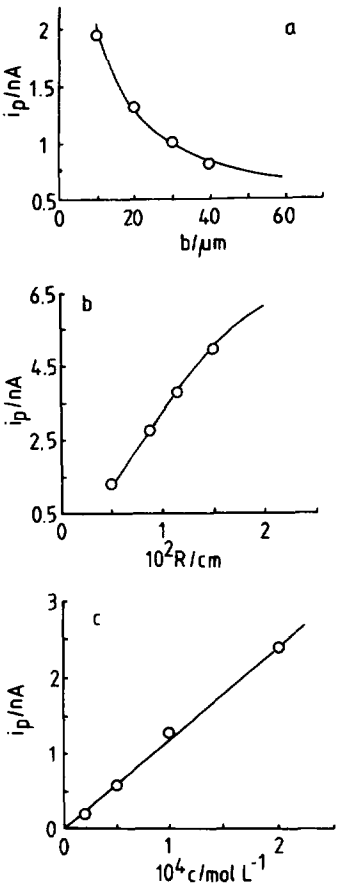

Fig. 5. Experimental (○) and theoretical (—) dependence of i_p on b, R and c. (a) $R = 5.00 \cdot 10^{-3}$ cm, $c = 1.00 \cdot 10^{-4}$ mol/l; (b) $b = 20$ μm, $c = 1.00 \cdot 10^{-4}$ mol/l; (c) $b = 20$ μm, $R = 5.00 \cdot 10^{-3}$ cm. $V_s = 9$ kV, $V_i = 1$ kV and $t_i = 3.0$ s. Other conditions as in Table 1.

5. Discussion

5.1.1. Influence of U, b, R and L_i on i_p

From Fig. 4, it can be seen that i_p increases almost linearly with increasing U and when $L_i < 0.2$ cm, i_p increases with increasing L_i; when $L_i > 0.2$ cm, i_p reaches a constant value. When $b > 10$ μm, the influence of b on i_p is obvious (Fig. 5a). The value of i_p increases with increasing radius of the disk working electrode. When $R < 150$ μm, the relation-

ship between i_p and R is almost linear (Fig. 5b). i_p is proportional to c (Fig. 5c), which is the foundation of the analytical application.

5.1.2. Simplified expression of i_p

According to the definition of the error function, the expression of

$$\mathrm{erf}\frac{L_i}{4\sqrt{Dt_m}}$$

is

$$\mathrm{erf}\frac{L_i}{4\sqrt{Dt_m}} = \frac{2}{\sqrt{\pi}}\int_0^{\frac{L_i}{4\sqrt{Dt_m}}} e^{-\eta^2}d\eta \qquad (11)$$

when

$$\frac{L_i}{4\sqrt{Dt_m}} < 0.4,\ \mathrm{erf}\frac{L_i}{4\sqrt{Dt_m}} \approx \frac{L_i}{2\sqrt{\pi Dt_m}}$$

with a relative standard deviation of 5%. Thus, Eq. (6) can be written as

$$i_p = \frac{1}{2}nFcU\frac{L_i}{\sqrt{\pi Dt_m}}\left[1 - m_1\exp\left(-\frac{m_2DA}{Ub}\right)\right] \qquad (12)$$

It was found that i_p is proportional to L_i. When

$$\frac{L_i}{4\sqrt{Dt_m}} > 2,\ \mathrm{erf}\frac{L_i}{4\sqrt{Dt_m}} = 1.$$

Eq. (6) can be written as

$$i_p = nFcU\left[1 - m_1\exp\left(1 - \frac{m_2DA}{Ub}\right)\right]$$
$$= nFcU\left[1 - m_1\exp\left(1 - \frac{m_2\pi DR^2}{Ub}\right)\right] \qquad (13)$$

In this case, i_p reaches a maximum, which is the same as the steady state current [29].

Acknowledgments

This project was supported by the National Science Foundation of China, the Science Foundation of Shandong Province and Laboratory of Electroanalytical Chemistry, Changchun Institute of Applied Chemistry, Chinese Academy of Sciences.

We thank Engineer Yifei Yu and Miss Xin Zhao for help with the experiments.

Appendix A

Derivation of Eq. (6). Eqs. (5a) (same as Eq. (5))

$$i = \frac{1}{2}nFcU\left[1 - m_1\exp\left(\frac{m_2DA}{Ub}\right)\right] \times\left[\mathrm{erf}\frac{\frac{L_i}{2} - (l - v_mt)}{2\sqrt{Dt}} + \mathrm{erf}\frac{\frac{L_i}{2} + (l - v_mt)}{2\sqrt{Dt}}\right] \qquad (5a)$$

Setting

$$K = \frac{1}{2}nFcU\left[1 - m_1\exp\left(\frac{m_2DA}{Ub}\right)\right] \qquad (A1)$$

and

$$f(t) = \mathrm{erf}\frac{\frac{L_i}{2} - (l - v_mt)}{2\sqrt{Dt}} + \mathrm{erf}\frac{\frac{L_i}{2} + (l - v_mt)}{2\sqrt{Dt}}, \qquad (A2)$$

we get

$$i = Kf(t) \qquad (A3)$$

Differentiating Eqs. (A3) with respect to t, one gets

$$\frac{di}{dt} = K\frac{df(t)}{dt} \qquad (A4)$$

Differentiating Eqs. (A2), we get

$$\frac{df(t)}{dt} = \frac{\left(l - \frac{L_i}{2}\right)t^{-3/2} + v_mt^{-1/2}}{4\sqrt{D}}\exp\left[-\frac{\left(\frac{L_i}{2} - l + v_mt\right)^2}{4Dt}\right] - \frac{\left(l + \frac{L_i}{2}\right)t^{-3/2} + v_mt^{-1/2}}{4\sqrt{D}}\exp\left[-\frac{\left(\frac{L_i}{2} + l - v_mt\right)^2}{4Dt}\right] \qquad (A5)$$

Substituting Eqs. (A5) into Eqs. (A4) and taking di/dt to be zero, we get

$$\frac{\left(l-\frac{L_i}{2}\right)t^{-3/2}+v_m t^{-1/2}}{4\sqrt{D}}\exp\left[-\frac{\left(\frac{L_i}{2}-l+v_m t\right)^2}{4Dt}\right]-\frac{\left(l+\frac{L_i}{2}\right)t^{-3/2}+v_m t^{-1/2}}{4\sqrt{D}}\exp\left[-\frac{\left(\frac{L_i}{2}+l-v_m t\right)^2}{4Dt}\right]=0 \quad \text{(A6)}$$

Multiplying by

$$4\sqrt{D}\,t^{3/2}\exp\left[\frac{\left(\frac{L_i}{2}-l+v_m t\right)^2}{4Dt}\right],$$

we obtain

$$l-\frac{L_i}{2}+v_m t=\left(l+\frac{L_i}{2}+v_m t\right)\exp\left[-\frac{L_i(l-v_m t)}{2Dt}\right] \quad \text{(A7)}$$

Since

$$l+v_m t \gg \frac{L_i}{2},$$

Eqs. (A7) can be written as

$$\exp\left[-\frac{L_i(l-v_m t)}{2Dt}\right]=1 \quad \text{(A8)}$$

The solution of Eqs. (A8) is

$$t=t_m=\frac{l}{v_m} \quad \text{(A9)}$$

When Eqs. (A9) is substituted into Eq. (5), $i=i_p$ and

$$i_p=nFcU\left[1-m_1\exp\left(-\frac{m_2 DA}{Ub}\right)\right]\mathrm{erf}\frac{L_i}{4\sqrt{Dt_m}}=nFcU\left[1-m_1\exp\left(-\frac{m_2\pi DR^2}{Ub}\right)\right]\mathrm{erf}\frac{L_i}{4\sqrt{Dt_m}} \quad \text{(6a)}$$

References

[1] F.E.P. Mikker, F.M. Everaerts and Th.P.E.M. Verheggen, J. Chromatgr., 169 (1979) 11.

[2] J.W. Jorgenson and K.D. Lukacs, J. Chromatogr., 218 (1981) 209.

[3] J.W. Jorgenson and K.D. Lukacs, Anal. Chem., 53 (1981) 1298.

[4] R.A. Wallingford and A.G. Ewing, Anal. Chem., 59 (1987) 1762.

[5] A.G. Ewing, R.A. Wallingford and T.M. Oleftrowicz, Anal. Chem., 61 (1989) 292A.

[6] Y.F. Yik and S.F.Y. Li, Trends Anal. Chem., 11 (1992) 325.

[7] P.D. Curry, Jr., C.E. Engstrom-Silverman and A.G. Ewing, Electroanalysis, 3 (1991) 587.

[8] A.G. Ewing, J.M. Mesaros and P.F. Gavin, Anal. Chem., 66 (1994) 527A.

[9] R.A. Wallingford and A.G. Ewing, Anal. Chem., 60 (1988) 258.

[10] R.A. Wallingford and A.G. Ewing, Anal. Chem., 61 (1989) 98.

[11] Y.F. Yik, H.K. Lee, S.F.Y. Li and S.B. Khoo, J. Chromatogr., 585 (1991) 139.

[12] T.J. O'Shea, R.D. Greenhagen, S.M. Lunte, C.E. Lunte, M.R. Smyth, D.M. Radzik and N. Watanabe, J. Chromatogr., 593 (1992) 305.

[13] T.J. O'Shea and S.M. Lunte, Anal. Chem., 65 (1993) 247.

[14] C.-W. Whang and I.-C. Chen, Anal. Chem., 64 (1992) 2461.

[15] T.J. O'Shea, S.M. Lunte and W.R. Lacoures, Anal. Chem., 65 (1993) 948.

[16] G. Li, B. Du, W. Jin, S. Wang, Q. Qu and W. Yu, Fenxi Huaxue (Chin. J. Anal. Chem.), 123 (1995) 480.

[17] W. Lu and R.M. Cassidy, Anal. Chem., 66 (1994) 200.

[18] X. Huang, R.N. Zare, S. Sloss and A.G. Ewing, Anal. Chem., 63 (1991) 189.

[19] W. Lu, R.M. Cassidy and A.S. Baranski, J. Chromatogr., 640 (1993) 433.

[20] W. Lu and R.M. Cassidy, Anal. Chem., 66 (1994) 200.

[21] S. Sloss and A.G. Ewing, Anal. Chem., 65 (1993) 577.

[22] J. Ye and R.P. Baldwin, Anal. Chem., 65 (1993) 3525.

[23] M. We and L. Xu, Fenxi Huaxue (Chin. J. Anal. Chem.), 23 (1995) 604.

[24] T.J. O'Shea and S.M. Lunte, Anal. Chem., 66 (1994) 307.

[25] W. Jin, H. Wei and X. Zhao, Anal. Chim. Acta, in press.

[26] W. Jin, Q. Weng and J. Wu, Anal. Lett., submitted.

[27] J. Crank, The Mathematics of Diffusion, Clarendon Press, Oxford, 2nd ed., 1975.

[28] S.G. Weber, in E.S. Yeung (Editor), Detectors for Liquid Chromatography, Wiley, New York, 1986, Ch. 7, p. 270.

[29] W. Jin and H. Chen, J. Electroanal. Chem., in press.

[30] I.M. Kolthoff and C. Barnum, J. Am. Chem. Soc., 62 (1940) 3061.

[31] M.T. Stankorich and A.J. Bard, J. Electroanal. Chem., 75 (1977) 487.

[32] W. Jin and Y. Wang, J. Chromatogr. A, in press.